# Near-wall streamwise turbulence intensity as $\mathrm{Re}_\tau \to \infty$

Yongyun Hwang*
*Department of Aeronautics, Imperial College London, South Kensington, London SW7 2AZ, United Kingdom*

(Received 4 March 2024; accepted 7 March 2024; published 2 April 2024)

In this study, asymptotic scaling of near-wall streamwise turbulence intensity $\overline{u'u'}/u_\tau^2$ ($u_\tau$ is the friction velocity) is theoretically explored. The three scalings previously proposed are first reviewed with their derivation and physical justification: (1) $\overline{u'u'}/u_\tau^2 \sim \ln \mathrm{Re}_\tau$ ($\mathrm{Re}_\tau$ is the friction velocity); (2) $\overline{u'u'}/u_\tau^2 \sim 1/U_\infty^+$ ($U_\infty^+$ is the inner-scaled freestream velocity in boundary layer); (3) $\overline{u'u'}/u_\tau^2 \sim \mathrm{Re}_\tau^{-1/4}$. A new analysis is subsequently developed based on velocity spectrum, and two possible scenarios are identified based on the asymptotic behavior of the outer-scaling part of the near-wall velocity spectrum. In the former case, the outer-scaling part of the spectrum is assumed to reach a nonzero constant as $\mathrm{Re}_\tau \to \infty$, and it results in the scaling of $\overline{u'u'}/u_\tau^2 \sim \ln \mathrm{Re}_\tau$, both physically and theoretically consistent with the classical attached eddy model. In the latter case, a sufficiently rapid decay of the outer-scaling part of the spectrum with Re is assumed due to the effect of viscosity, such that $\overline{u'u'}/u_\tau^2 < \infty$ for all $\mathrm{Re}_\tau$. The following analysis yields $\overline{u'u'}/u_\tau^2 \sim 1/\ln \mathrm{Re}_\tau$, asymptotically consistent with the scaling of $\overline{u'u'}/u_\tau^2 \sim 1/U_\infty^+$. The scalings are further verified with the existing simulation and experimental data and those from a quasilinear approximation [Holford *et al.* J. Fluid Mech. **980**, A12 (2024)], the spectra of which all appear to favor $\overline{u'u'}/u_\tau^2 \sim 1/\ln \mathrm{Re}_\tau$, although new datasets for $\mathrm{Re}_\tau \gtrsim O(10^4)$ would be necessary to conclude this issue.

DOI: 10.1103/PhysRevFluids.9.044601

## I. INTRODUCTION

The first-order moment (mean) of streamwise velocity of wall-bounded turbulence has a well-established layered structure in the wall-normal direction. In particular, in the near-wall region, the mean streamwise velocity is expressed in terms of a Reynolds-number-independent universal function, when normalized by the kinematic viscosity $\nu$ and the friction velocity $u_\tau$: i.e., the law of the wall [1]. Early studies speculated that the second-order moment of the near-wall streamwise velocity would also behave in the same way [e.g., Refs. [2,3]]. However, a large number of datasets, taken from accurate laboratory experiments and direct numerical simulations (DNS) since the 1990s, have revealed that the near-wall peak streamwise turbulence intensity consistently grows with Reynolds number. Figure 1 reports the near-wall peak streamwise turbulence intensity in a range of the friction Reynolds number $\mathrm{Re}_\tau$ from a number of previous experiments and DNSs [e.g., Refs. [4–20], and many others]. Although the data are relatively scattered due to different flow geometry, experimental measurement methods, and numerical simulation methods, it is seen that

*y.hwang@imperial.ac.uk

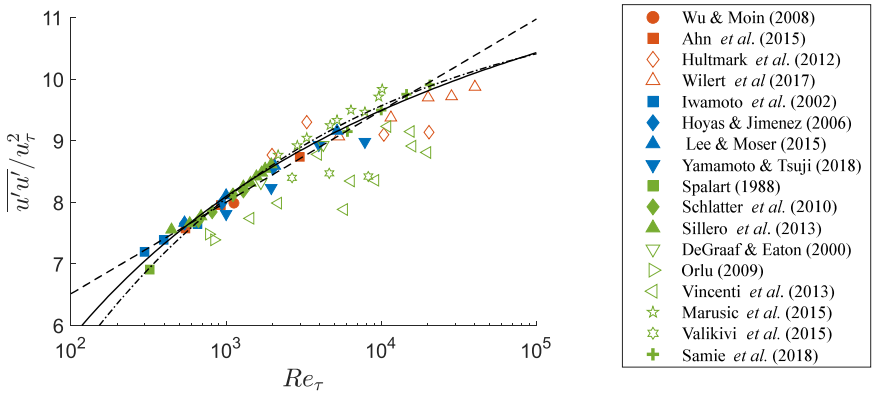


FIG. 1. Peak streamwise turbulence intensities from experiments (open symbols) and DNSs (filled symbols) and their scaling laws: - - - -, $A_S + B_S \ln \mathrm{Re}_\tau$, with $A_S = 0.646$ and $B_S = 3.54$ [20]; ——, $A_M - B_M/U_\infty^+$, with $A_M = 15.2$ and $B_M = 174$, where the free stream velocity $U_\infty$ is given by $U_\infty^+ = (1/\kappa)\ln \mathrm{Re}_\tau + 6.5$, with $\kappa = 0.384$ (note $A_M$ and $B_M$ here are different from those proposed in Refs. [21,22], where an error was found in the description of $U_\infty^+$); – – – –, $A_C + B_C \ln \mathrm{Re}_\tau$, with $A_C = 11.5$ and $B_C = 19.32$ [23]. The data from pipe, channel, and boundary layer are denoted by the orange, blue and green colors, respectively. Here, $\overline{(\cdot)}$ indicates a time average and the superscript $(\cdot)^+$ denotes the inner-scaling with $u_\tau$ and $\nu$.

the near-wall peak streamwise turbulence intensity grows slowly at least within the range of $\mathrm{Re}_\tau$ considered.

The present study concerns the issue of how the growth of the peak intensity asymptotically scales as $\mathrm{Re}_\tau \to \infty$. There are three different scaling laws that have been proposed so far: (1) $\ln \mathrm{Re}_\tau$ scaling [24]; (2) Inverse of $U_\infty^+$ scaling ($U_\infty$ is the freestream velocity in boundary layer and the superscript $(\cdot)^+$ denotes the inner-scaling with $u_\tau$ and $\nu$) [21]; (3) $\mathrm{Re}_\tau^{-1/4}$ scaling [23]. As seen in Fig. 1, the three different scaling laws appear to be all reasonably good with the existing data, when the fitting constants are appropriately chosen, leading this issue to be unsettled without very accurate data available at higher $\mathrm{Re}_\tau$. This paper will therefore begin first by reviewing these scaling laws with focus on their derivation, supporting evidence, limitations, and physical relevance.

### A. $\ln \mathrm{Re}_\tau$ scaling

From their experimental data in a turbulent boundary layer, the authors of Ref. [7] observed that $\overline{u'u'}/u_\tau^2$ slowly grows with $\mathrm{Re}_\tau$ in a way that $\overline{u'u'}/u_\tau U_\infty$ remains approximately constant. Given that $U_\infty^+ \sim \ln \mathrm{Re}_\tau$ at high $\mathrm{Re}_\tau$, this also approximately implies the following scaling:

$$\left.\frac{\overline{u'u'}}{u_\tau^2}\right|_{y^+=y_p^+} = A_S + B_S \ln \mathrm{Re}_\tau, \tag{1}$$

where $y_p^+$ is the peak wall-normal location, and $A_S$ and $B_S$ are appropriate constants to be chosen. Reference [24] pointed out that this observation is consistent with the classical attached eddy model [25–27], when the near-wall streamwise velocity fluctuation is modeled to be

$$\frac{\overline{u'u'}(y^+)}{u_\tau^2} = f_1(y^+) + f_2(y/\delta), \tag{2a}$$

where

$$f_2(y/\delta) = A_1 - B_1 \ln\left(\frac{y}{\delta}\right), \tag{2b}$$

with $\delta$ being the outer length scale, such as half height of channel, radius of pipe, and thickness of boundary layer. Here, $f_1(y^+)$ is a universal inner-scaling function which describes the streamwise

turbulence intensity only from the viscous inner-scaling motions, and $f_2(y/\delta)$ depicts the contribution from the logarithmic and outer regions given by the classical attached eddy model [25], where $B_1$ has often been referred to as the Townsend-Perry constant [28]. Note that if the peak location is assumed to be constant (say $y_p^+ = 15$), $\overline{u'u'}/u_\tau^2$ at the peak would be proportional to $\ln \mathrm{Re}_\tau$ with $B_S = B_1 \ln y_p^+$ as in Eq. (1). Given that the Townsend-Perry constant proposed was $B_1 \simeq 1.26$ [e.g., Ref. [28]], (2) would yield $B_S = 3.41$, not very far from $B_S = 3.54$ proposed by Ref. [20] from their measurement of the peak intensity.

Perhaps, the scaling in Eq. (1) has been employed most commonly, as there is a considerable amount of evidence supporting the attached eddy hypothesis: i.e., the existence of the self-similar energy-containing motions, the size of which is proportional to the distance from the wall in the logarithmic region (see also the recent review in Ref. [29]). The attached eddy hypothesis itself has recently been demonstrated theoretically in terms of energetics [30], and there has been firm evidence on the existence of self-similar energy-containing eddies [31–40] as well as supporting mathematical structure from the Navier-Stokes equations [41–47].

The existence of the self-similar energy-containing motions in the logarithmic layer does not, however, necessarily imply that Eq. (2) is without any issues. Note that Eq. (2b) is supposed to be valid in the logarithmic layer in the limit of $\mathrm{Re}_\tau \to \infty$. It is also obtained by assuming that each of the self-similar energy-containing motions satisfies slip boundary condition (i.e., an inviscid theory), the key mathematical feature required to have the logarithmic term in Eq. (2b) [25]. However, any fluid motions in a viscous fluid must satisfy no-slip boundary condition, and the viscous effect is important in the near-wall region, where the scaling of interest concerns. In fact, Ref. [48] showed that there is nontrivial Reynolds-number dependent viscous effect on the spectra of the footprint of self-similar energy-containing motions (i.e., the near-wall part of the motions). Even in the entire logarithmic layer, the viscous effect is not negligible as long as $\mathrm{Re}_\tau$ is finite. In the upper logarithmic layer (or inertial sublayer), it was recently shown that both $A_1$ and $B_1$ must vary with $\mathrm{Re}_\tau$ theoretically [49]. In the lower logarithmic layer (or mesolayer) [42,50], an expression different from Eq. (2b) is needed to incorporate the viscous effect: for example, see Eq. (4.6) in Ref. [49].

### B. Inverse of $U_\infty^+$ scaling

Reference [21] proposed a scaling of near-wall peak streamwise turbulence with $\mathrm{Re}_\tau$ different from Eq. (1). The proposed scaling reads as

$$\left.\frac{\overline{u'u'}}{u_\tau^2}\right|_{y^+=y_p^+} = A_M + \frac{B_M}{U_\infty^+} + O\left(\frac{1}{U_\infty^{+2}}\right), \tag{3}$$

where $A_M$ and $B_M$ are constants. The scaling Eq. (3) is obtained by an asymptotic analysis of streamwise mean momentum equation of turbulent boundary layer combining with the existing DNS data. Using the von Kármán integral momentum equation, Ref. [21] showed that the small parameter required for the asymptotic balance would be $1/U_\infty^+$. The resulting $\overline{u'u'}/u_\tau^2$ is then finite at $\mathrm{Re}_\tau \to \infty$ and proportional to $1/U_\infty^+$ for sufficiently high $\mathrm{Re}_\tau$.

The scaling Eq. (3) provides a good fit for the existing dataset (solid line in Fig. 1) (see also Ref. [51]). It is also obtained by a direct analysis of the Navier-Stokes equations using DNS data unlike the one in Ref. [24], where a model for flow field is employed (i.e., the attached eddy model). It is, however, strictly applicable to boundary layers, where the mean momentum equation contains nonvanishing $\overline{u'u'}$; for example, $\overline{u'u'}$ does not appear in the streamwise mean momentum equation in internal parallel shear flows, such as channel and pipe, thereby not being able to straightforwardly justify Eq. (3) for such flows. Nevertheless, recent studies, which applied quasilinear approximations to the Navier-Stokes equations in channel flow [52–54], have also shown that their peak streamwise turbulence intensity consistently follows the scaling in Eq. (3), although the underlying mathematical reason remains not understood.

### C. $\mathrm{Re}_\tau^{-1/4}$ scaling

The final scaling of interest in this study has recently been proposed by Ref. [23]:

$$\left.\frac{\overline{u'u'}}{u_\tau^2}\right|_{y^+=y_p^+} = A_C + B_C \mathrm{Re}_\tau^{-1/4} + O(y^{+3}), \tag{4}$$

where $A_C$ and $B_C$ are constants to be determined with the measured data. The starting point of Eq. (4) is from the following equation, obtained by applying a Taylor expansion about the wall:

$$\frac{\overline{u'u'}(y)}{u_\tau^2} = \epsilon_W^+ y^{+2} + O(y^{+3}), \tag{5}$$

where $\epsilon_W^+$ is inner-scaled turbulence dissipation at the wall. Two key conjectures are subsequently made to estimate the scaling behavior of $\overline{u'u'}/u_\tau^2$ in the near-wall region. First, from the well-known fact that the inner-scaled turbulence production is bounded by $1/4$ as $\mathrm{Re}_\tau \to \infty$, Ref. [23] argued that $\epsilon_W^+$ is also expected to be bounded by $\epsilon_\infty^+ (= 1/4)$. The defect dissipation from this bound, $\epsilon_d$, may be defined as

$$\epsilon_d^+ = 1/4 - \epsilon_W^+. \tag{6a}$$

Second, it was also argued that the defect dissipation may be related to bursting in the near-wall region [e.g., Ref. [55]], which transports some of the turbulent kinetic energy to the outer region without being dissipated locally. The timescale of this process is subsequently hypothesized to be $\eta_o/u_\tau$, where $\eta_o$ is the Kolmogorov length scale in the outer region: i.e., $\eta_0 = \nu^{3/4}/\epsilon_o^{1/4}$, where $\epsilon_o = u_\tau^3/\delta$. If this is so, then $\epsilon_d^+ \sim \mathrm{Re}^{-1/4}$. Combining with Eq. (8), this leads to

$$\epsilon_W^+ = 1/4 - \beta \mathrm{Re}_\tau^{-1/4}, \tag{6b}$$

where $\beta$ is a constant to be determined.

The scaling Eq. (5) provides a good fit for the existing dataset (dash-dotted line in Fig. 1). However, apart from the influence of the higher-order term in Eq. (5), unfortunately, the two conjectures made to derive Eq. (5) in Ref. [23] do not have supporting evidence. First, there is no physical reason for $\epsilon_W^+$ to be bounded by the peak near-wall production, $1/4$. Wall-bounded turbulence is largely nonlocal in the wall-normal direction, and there is a large amount of evidence that the near-wall region is subject to influence of the structures originating from the logarithmic and the outer regions [see Refs. [56–61], and many others]. Importantly, the turbulent energy transport caused by the resulting near-wall inner-outer interaction is directly balanced with dissipation in the near-wall region [62]. In other words, unlike the production only affected by inner scale [see the Reynolds shear stress spectra (Fig. 10(e)) in Ref. 48], dissipation in the near-wall region is increasingly influenced by the wall-attached part of the energy-containing motions from the log- and outer regions upon increasing $\mathrm{Re}_\tau$. This implies that $\epsilon_W^+$ needs not to be bounded by the peak production value $1/4$ in the limit of $\mathrm{Re}_\tau \to \infty$—it is possible for the near-wall region to dissipate out the near-wall part of structures associated with infinitely many scales varying from $\delta_\nu (\equiv \nu/u_\tau)$ to $\delta$, given that $\mathrm{Re}_\tau = \delta/\delta_\nu$ by definition. In fact, we shall see in Sec. II that the increase of the near-wall peak intensity with $\mathrm{Re}_\tau$ is because there is an increasing contribution of the wall-attached part of the motions originating from the log- and outer regions (Fig. 3), a physical picture rather consistent with attached eddy hypothesis [25].

Second, there is no evidence that bursting transports the near-wall turbulence all the way up to the outer region especially for $\mathrm{Re}_\tau \to \infty$. In fact, it is quite possible that the near-wall turbulence transported upwards by bursting may well be dissipated in the logarithmic region, where most of dissipation should take place at high $\mathrm{Re}_\tau$ [63]: see also data from Refs. [18,64]. Let us assume that the transport process takes place at the timescale of $\eta_o/u_\tau$, as conjectured by Ref. [23]. Given that $v \sim O(u_\tau)$ throughout the entire wall-normal location ($v$ is the wall-normal velocity), the wall-normal turbulent transport (or the wall-normal advective flux for turbulent fluctuation) can take place only with the speed of $O(u_\tau)$. The distance that the near-wall turbulence can travel upwards is then

only $O(\eta_o)$ over the timescale of $O(\eta_o/u_\tau)$. Given $\eta_o/\delta = \mathrm{Re}_\tau^{-3/4}$, it is evident that the near-wall turbulence is increasingly unable to reach the outer region as $\mathrm{Re}_\tau \to \infty$. It will remain at best in the lower logarithmic region (or mesolayer), given that $\delta_m/\delta \sim \mathrm{Re}_\tau^{-1/2}$ ($\delta_m$ is the upper boundary of the mesolayer [50,65]). This suggests that the second conjecture of Ref. [23] is self-contradictory. More importantly, in the spanwise minimal channel [66], where the bursting is allowed to transport near-wall turbulence from the wall in the absence of the motions from the logarithmic and outer regions, the near-wall streamwise turbulence intensity does not change with $\mathrm{Re}_\tau$, not supporting the second conjecture of Ref. [23].

### D. Scope of the present study

Thus far, the relevance of the three scalings of the near-wall peak streamwise turbulence intensity has been reviewed. The scaling in Eq. (1) has a good physical grounds as a large number of recent investigations have confirmed the existence of statistically and dynamically self-similar energy-containing motions in the logarithmic layer (i.e., attached eddies). However, it remains unclear if the simple extension of the classical attached eddy model described in Eq. (2) would accurately incorporate the near-wall viscous effect into streamnwise turbulence intensity. The scaling in Eq. (3) is rigorous and self-consistent at least for boundary layer, as Eq. (3) is directly derived from an asymptotic analysis of the Naiver-Stokes equations [21]. Nevertheless, the physical implication of this scaling is unclear especially in relation to the dynamics of the flow (e.g., coherent structures, energy balance, etc). Last, the scaling Eq. (5) does not appear to have strong physical grounds, as the two main hypotheses set up are too speculative and allow for some critical counter-arguments with a room for a further debate.

Given the discussion above on the three different scaling laws, the objective of the present study is to theoretically explore the possible asymptotic scaling behaviors of near-wall streamwise turbulence intensity as $\mathrm{Re}_\tau \to \infty$. In Sec. II, some observations will first be made on the near-wall streamwise velocity and corresponding spectrum with DNS [18] and experimental [20] data. Based on this observation, an exact form of the near-wall streamwise turbulence intensity is formulated using a dimensional analysis of the corresponding velocity spectra. In Sec. III, it will be seen that the near-wall spectrum for $k_x\delta \sim O(1)$ ($k_x$ is the streamwise wave number) has a crucial importance in the prediction of scaling. Depending on its behavior, two scaling behaviors will be shown to be possible: (1) $\overline{u'u'}/u_\tau^2 \sim \ln \mathrm{Re}_\tau$; (2) $\overline{u'u'}/u_\tau^2 \sim (\ln \mathrm{Re}_\tau)^{-1}$. The near-wall spectra from the existing DNS [18] and experimental data [20] will be seen to favor the latter case at least within the range of $Re_\tau$ currently available. In Sec. IV, a summary will first be given and the relevance of the latter scaling will be discussed further using the data generated by a quasilinear approximation of the Navier-Stokes equations for channel flow up to $\mathrm{Re}_\tau = 10^5$ [54].

## II. PROBLEM FORMULATION

### A. Some observations on near-wall turbulence intensity

Before exploring the possible scaling behavior, it would be useful to start by making some observations on the features of near-wall turbulence intensity. Figure 2 shows the behavior of near-wall streamwise turbulence intensity in channel flow from Ref. [18] on increasing $\mathrm{Re}_\tau$. The growth of the near-wall turbulence intensity is evident over the entire near-wall region, as seen in Fig. 2(a). The peak wall-normal location appears at $y^+_{\mathrm{peak}} \simeq 15$, but there is also a very weak dependence on $\mathrm{Re}_\tau$, the feature also pointed out by some previous studies [e.g., Refs. [19,52]]. Note that all the three scalings discussed in Sec. I assume the inner-scaled peak location is not a function of $\mathrm{Re}_\tau$. Although the derivation of Eq. (3) could suitably be modified without change in its form (see Sec. III B), Fig. 2(a) implies that, in principle, comparing the peak streamwise turbulence intensity from DNS/experimental data with all the three scalings discussed in Sec. I is not precisely valid, especially when a wide range of $\mathrm{Re}_\tau$ encompassing several decades is to be considered. Instead, the streamwise turbulence intensity at a fixed inner-scaled wall-normal location must be considered

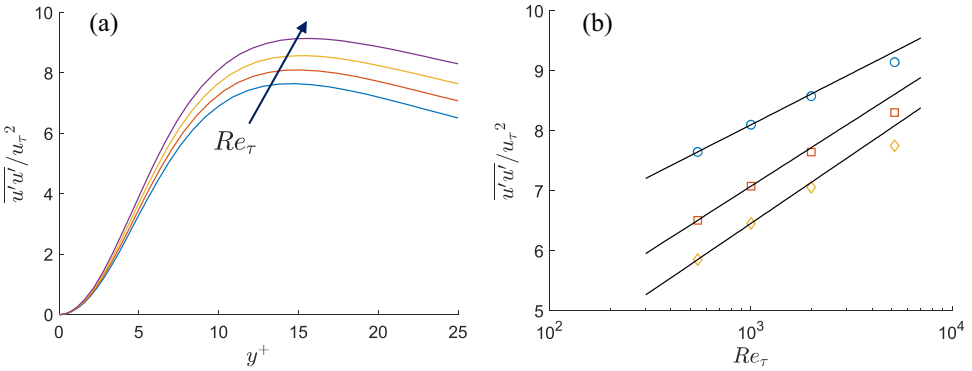


FIG. 2. Near-wall streamwise turbulence intensity in channel for $\mathrm{Re}_\tau = 544, 1000, 1995, 5186$ [18]: (a) near-wall profile of $\overline{u'u'}(y^+)/u_\tau^2$; (b) values of $\overline{u'u'}(y^+)/u_\tau^2$ at $y^+ = y^+_{\mathrm{peak}}, 25, 30$ with $y^+_{\mathrm{peak}} \simeq 15$. In panel (b), the solid black lines indicate fits in the form of $A \log \mathrm{Re}_\tau + B$, where $A$ and $B$ are determined by the data at two lowest Reynolds numbers.

to be directly compared with the scalings given in Sec. I. Figure 2(b) shows the scaling behavior of near-wall turbulence intensity at a few more locations in the near-wall region. It becomes more evident even at relatively low $\mathrm{Re}_\tau(\lesssim 5200)$ that the near-wall turbulence intensity deviates from Eq. (1), indicating that the DNS data favors the alternative scalings, Eq. (3) or Eq. (4).

To understand the behavior of near-wall streamwise turbulence intensity in Fig. 2 better, we consider its power spectral density with respect to the streamwise wave number $k_x$, defined with

$$\overline{u'u'}(y) = \int_0^\infty \Phi_{uu}(k_x, y) dk_x = \int_{-\infty}^\infty k_x \Phi_{uu}(k_x, y) d(\ln k_x). \tag{7}$$

Figure 3 visualizes premultiplied power spectral density of streamwise velocity at $y^+ = 15$ with respect to inner- and outer-scaled streamwise wave number. Here, the data are from Ref. [18] for channel [Figs. 3(a) and 3(b)] and from Ref. [20] for boundary layer [Figs. 3(c) and 3(d)]. When each spectrum from different $\mathrm{Re}_\tau$ is scaled with inner units [Figs. 3(a) and 3(c)], all of them collapse into a single curve with the maximum intensity of $k_x^+ \Phi_{uu}^+(k_x^+) \simeq 2.2$ for $k_x^+ \gtrsim O(10^{-3})$ $[\lambda_x^+ \lesssim O(10^3)$ where $\lambda_x = 2\pi/k_x]$. In particular, the peak occurs at $k_x^+ \simeq 0.007$ $(\lambda_x^+ \simeq 1000)$, close to the streamwise length of near-wall streaks [66]. As $\mathrm{Re}_\tau$ is increased, the spectrum gradually extends to smaller $k_x^+$, forming a long tail at $k_x^+ \lesssim O(10^{-3})$ for $\mathrm{Re}_\tau$ considered here. The presence of the spectral tail for small $k_x$ (or large $\lambda_x$) is evidently the reason why the peak streamwise turbulence intensity grows with $\mathrm{Re}_\tau$.

Given that the largest length scale of the flow is $\delta$, the spectra with respect to the outer-scaled streamwise wave number are further plotted in Figs. 3(c) and 3(d). Both DNS and experimental data show that there is a considerable amount of spectral energy at $k_x\delta \lesssim 1$ $(\lambda_x/\delta \gtrsim 2\pi)$. As discussed in Sec. I, this is associated with the penetration of very large-scale motions (or $\delta$-scaling long streaky motions) into the near-wall region [56–61]. Note that the spectral energy at this wave number range decays with $\mathrm{Re}_\tau$, suggesting that the near-wall influence (or footprint) of $\delta$-scaling long streaky motions appears to diminish. This is the nontrivial viscous wall effect on the footprint of $\delta$-scaling structures [48], and its origin currently remains not understood. Assuming a gradual diminishment of energy for $k_x\delta \lesssim 1$ on increasing $\mathrm{Re}_\tau$, most of the spectral energy related to the growth of $\overline{u'u'}/u_\tau^2$ with $\mathrm{Re}_\tau$ is expected to originate from $O(1/\delta) \lesssim k_x \lesssim O(1/\delta_\nu)$, as $\mathrm{Re}_\tau \to \infty$. By definition, these streamwise wave numbers (or length scales) are associated with the logarithmic layer (i.e., the overlap region). Indeed, the near-wall spectral energy for $O(1/\delta) \lesssim k_x \lesssim O(1/\delta_\nu)$ has consistently been understood to be the contribution of "inactive" motions of self-similar attached eddies of Ref. [25] [for a detailed discussion, see also Refs. [35,48,67,68]]. It is worth mentioning that the

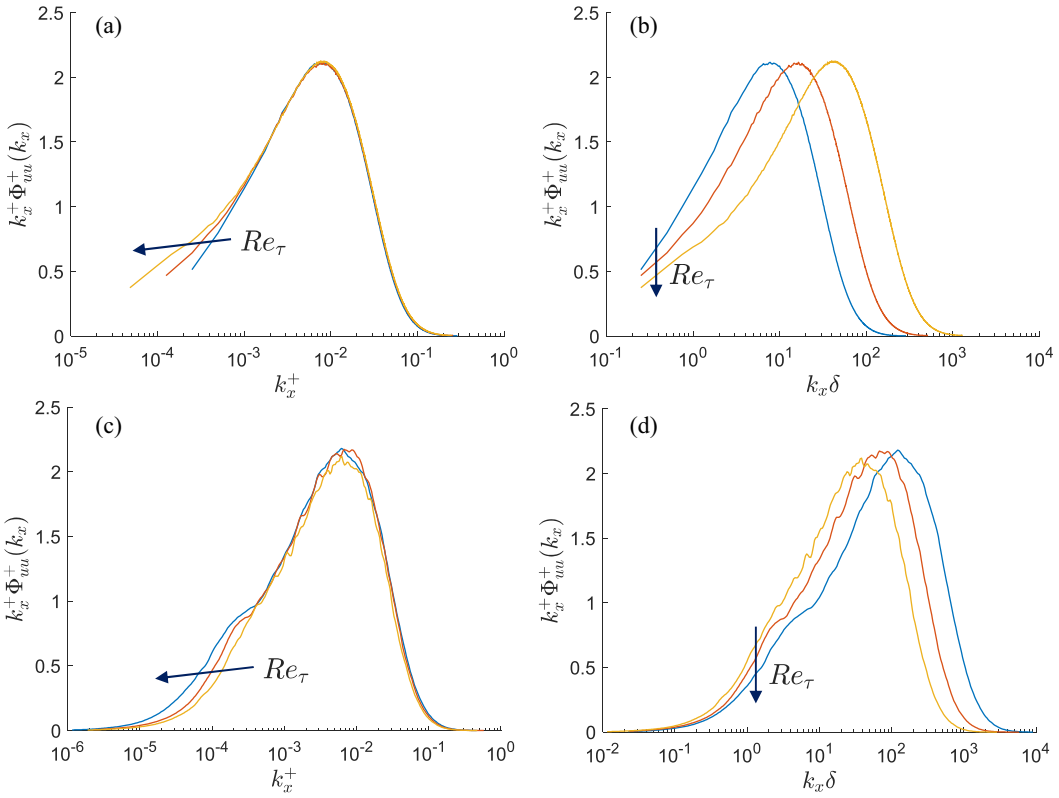


FIG. 3. Premultiplied streamwise wave number spectra of streamwise velocity at $y^+ = 15$ in panels (a), (b) channel [DNS from [18]] and in panels (c), (d) boundary layer [experiment from Ref. [20]]: (a), (c) inner scaling; (b), (d) outer scaling. In panels (a), (b), $\mathrm{Re}_\tau = 1000, 1995, 5186$, and, in panels (c), (d), $\mathrm{Re}_\tau = 6123, 10\,100, 19\,680$.

logarithmic term in the scaling of Eq. (1) theoretically originates from such inactive motions, the consequence of allowing for wall-parallel fluid motions near the wall through the slip boundary condition [25]. In this respect, the scaling in Eq. (1) is still sound with DNS and experimental data at least from a physical viewpoint, although the poorly understood viscous effect presumably undermines its precise relevance to viscous fluids.

### B. Near-wall turbulence intensity

Given the discussion in Sec. II A, the behavior of the streamwise velocity spectrum in the near-wall region is crucial to understand the peak scaling of $\overline{u'u'}/u_\tau^2$ with $\mathrm{Re}_\tau$. Here, a further analysis will be presented for the streamwise wave number velocity spectrum, a function of $u_\tau$, $\nu$ and $\delta$, $k_x$, and $y$. A schematic diagram of the spectrum is first considered at a fixed inner-scaled wall-normal location (i.e., $y^+ = c$) close to the peak location of $\overline{u'u'}/u_\tau^2$, as in Fig. 4. The structure of spectrum is set to be divided into three regions, depending on the value of $k_x$: (1) Region I, where $k_x \lesssim O(1/\delta)$; (2) Region II, where $k_x \gtrsim O(1/\delta_\nu)$; (3) Region III, where $O(1/\delta) \lesssim k_x \lesssim O(1/\delta_\nu)$.

Region I is defined to be $k_x\delta \leqslant a$ ($a$ is an appropriate constant to be chosen from data) at a fixed inner-scaled wall-normal location (say $y^+ = c$), leading to $k_x \sim O(1/\delta)$ and $y \sim O(\delta_\nu)$. Combining this with the Buckingham $\Pi$ theorem and Eq. (7), the spectrum is given by

$$\frac{\Phi_{uu}(k_x, y; \delta, \delta_\nu)}{u_\tau^2} = \frac{\delta\Phi_{uu}(k_x\delta, y^+; \mathrm{Re}_\tau)}{u_\tau^2} = \delta g_1(k_x\delta, y^+; \mathrm{Re}_\tau). \tag{8a}$$

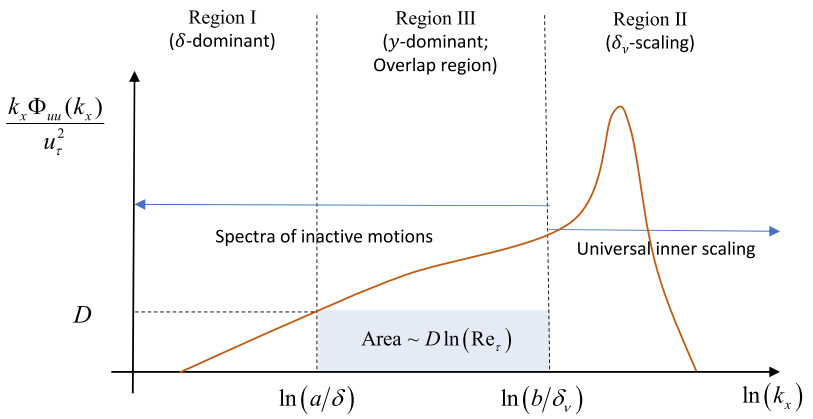


FIG. 4. A schematic diagram of the premultiplied one-dimensional spectrum of near-wall streamwise velocity at a fixed inner-scaled wall-normal location ($y^+ = c$).

At $y^+ = c$, the corresponding dimensionless premultiplied spectrum is then written as

$$\frac{k_x \Phi_{uu}(k_x; \delta, \delta_\nu)}{u_\tau^2} = \frac{k_x \delta \Phi_{uu}(k_x \delta; \mathrm{Re}_\tau)}{u_\tau^2} = k_x \delta g_1(k_x \delta; \mathrm{Re}_\tau) = h_1(k_x \delta; \mathrm{Re}_\tau). \tag{8b}$$

Now, it becomes evident that the dimensionless premultiplied spectrum for $k_x \delta \sim O(1)$ must be a function of $\mathrm{Re}_\tau$ in general, consistent with the DNS and experimental data shown in Figs. 3(a) and 3(b).

Similarly to Region I, Region II is defined at $y^+ = c$ for $k_x^+ \geqslant b$, where $b$ is an appropriate constant, yielding $k_x \sim O(1/\delta_\nu)$ and $y \sim O(\delta_\nu)$. It is therefore expected that $\delta$ would no longer be relevant in Region II. It is also worth noting that $\delta_\nu$ is the Kolmogorov length scale in the near-wall region, as the dissipation rate is given by $\epsilon = u_\tau^3/\delta_\nu$. This implies that the smallest possible length scale of the spectrum is $\delta_\nu$ and that turbulence production and dissipation takes place at the same length scale in the near-wall region, like in typical transitional flows. Therefore, it is expected that there is no spectrum developed for energy cascade (i.e., the $k_x^{-5/3}$ law) in Region II. The Buckingham $\Pi$ theorem and Eq. (7) subsequently lead the spectrum to take the following form:

$$\frac{\Phi_{uu}(k_x, y; \delta_\nu)}{u_\tau^2} = \frac{\delta_\nu \Phi_{uu}(k_x^+, y^+)}{u_\tau^2} = \delta g_2(k_x \delta, y^+). \tag{9a}$$

The corresponding dimensionless premultiplied spectrum at $y^+ = c$ is given by

$$\frac{k_x \Phi_{uu}(k_x)}{u_\tau^2} = \frac{k_x^+ \Phi_{uu}(k_x^+)}{u_\tau^2} = k_x^+ g_2(k_x^+) = h_2(k_x^+). \tag{9b}$$

Unlike Eq. (8b), the spectrum in Region II does not have any dependence on $\mathrm{Re}_\tau$, since $\delta$ is a length no longer relevant scale here. This is consistent with the DNS and experimental data in Figs. 3(a) and 3(c), where the spectra from different $\mathrm{Re}_\tau$ are collapsed into a single curve.

Region III is defined for $a/\delta \leqslant k_x \leqslant b/\delta_\nu$. If $h_1(k_x \delta; \mathrm{Re}_\tau)$ and $h_2(k_x^+)$ are known, then an asymptotic matching may be proceeded to understand the form of the spectrum for $O(1/\delta) \ll k_x \ll O(1/\delta_\nu)$ as in Ref. [27] for the logarithmic layer. It will be seen in Sec. III A that such an analytical progress is possible for a particular case without knowing the full details of $h_1(k_x \delta; \mathrm{Re}_\tau)$ and $h_2(k_x^+)$. However, in general, the dimensionless premultiplied spectrum in Region III is expected to be a function of $\mathrm{Re}_\tau$, given that the spectrum in Region I is a function of $\mathrm{Re}_\tau$; i.e.,

$$\frac{k_x \Phi_{uu}(k_x)}{u_\tau^2} = h_3(k_x l; \mathrm{Re}_\tau), \tag{10}$$

where $l$ is an appropriate length scale given by $\delta_\nu < l < \delta$.

Using Eq. (7) and the features of the spectra from Eqs. (8) to (10), the streamwise turbulence intensity at $y^+ = c$ may be written as follows:

$$\left.\frac{\overline{u'u'}}{u_\tau^2}\right|_{y^+=c} = \underbrace{\int_{-\infty}^{\ln(a/\delta)} \frac{k_x \Phi_{uu}(k_x, c\delta_\nu)}{u_\tau^2} d(\ln k_x)}_{\text{Region I}} + \underbrace{\int_{\ln(b/\delta_\nu)}^{\infty} k_x \Phi_{uu}(k_x, c\delta_\nu) d(\ln k_x)}_{\text{Region II}}$$
$$+ \underbrace{\int_{\ln(a/\delta)}^{\ln(b/\delta_\nu)} \frac{k_x \Phi_{uu}(k_x, c\delta_\nu)}{u_\tau^2} d(\ln k_x)}_{\text{Region III}}$$
$$= A(\mathrm{Re}_\tau) + C + B(\mathrm{Re}_\tau)\left[\ln \mathrm{Re}_\tau + \ln\left(\frac{b}{a}\right)\right], \tag{11a}$$

where

$$A(\mathrm{Re}_\tau) = \int_{-\infty}^{\ln a} h_1(k_x\delta; \mathrm{Re}_\tau) d(\ln(k_x\delta)) \tag{11b}$$

from Region I,

$$C = \int_{\ln b}^{\infty} h_2(k_x^+) d(\ln k_x^+) \tag{11c}$$

from Region II, and

$$B(\mathrm{Re}_\tau) = \left[\ln\left(\frac{bl}{\delta_\nu}\right) - \ln\left(\frac{al}{\delta}\right)\right]^{-1} \int_{\ln(al/\delta)}^{\ln(bl/\delta_\nu)} h_3(k_x l; \mathrm{Re}_\tau) d(\ln(k_x l)) \tag{11d}$$

from Region III. Here, the value of $B(\mathrm{Re}_\tau)$ must be comparable to a typical value of dimensionless premultiplied power-spectral intensity for $a/\delta \leqslant k_x \leqslant b/\delta_\nu$, because the mean value theorem for integral indicates the existence of $B(\mathrm{Re}_\tau)$, satisfying

$$B(\mathrm{Re}_\tau) = h_3(k_x^* l; \mathrm{Re}_\tau), \tag{11e}$$

where $k_x^*$ is a streamwise wave number given in the range of $a/\delta \leqslant k_x^* \leqslant b/\delta_\nu$.

It is also worth noting that $a$ and $b$ are appropriate constants to be chosen. While the choice for $b$ must ensure $C$ in Eq. (11c) to be a constant, the choice for $a$ is rather arbitrary as long as $a \lesssim O(1)$. In fact, choosing a sufficiently small $a(\ll 1)$ can further simplify (11) into

$$\left.\frac{\overline{u'u'}}{u_\tau^2}\right|_{y^+=c} = C + B(\mathrm{Re}_\tau)\left[\ln \mathrm{Re}_\tau + \ln\left(\frac{b}{a}\right)\right] + O(a^2), \tag{12a}$$

where the contribution from Region I [i.e., $A(\mathrm{Re}_\tau)$] is estimated to be

$$A(\mathrm{Re}_\tau) = \int_0^{a/\delta} \frac{\Phi_{uu}(k_x)}{u_\tau^2} d(k_x) = \int_0^{a} \frac{\Phi_{uu}(k_x\delta)}{u_\tau^2} d(k_x\delta) \sim O(a^2) \tag{12b}$$

from $\Phi_{uu}(k_x\delta) \sim k_x\delta$ for $k_x\delta \ll 1$. For example, if $a = 0.01$ is chosen for the experimental data of Ref. [20], then $A(\mathrm{Re}_\tau) \sim O(10^{-4})$ and this is seen to be negligibly small [Fig. 3(d)]. However, such a small choice of $a$ does not lead to any singular behavior of $\ln(b/a)$ in Eq. (12a) because of its logarithm. Indeed, if $b = 10^{-3}$ is chosen with $a = 0.01$ from the data in Figs. 3(a) and 3(c), then $\ln(b/a) \sim O(1)$.

## III. TWO POSSIBLE SCENARIOS

The formulation in Sec. II B suggests that the increase of $\overline{u'u'}/u_\tau^2$ in the near-wall region is due to the increasing contribution of the motions, the streamwise length scale of which varies from $\delta_\nu$

to $\delta$. From a physical viewpoint, this is consistent with the underlying rationale in the derivation of Eq. (1). In this section, a further progress from Eq. (11) or alternatively from Eq. (12) will be sought by considering two scenarios associated with the $\mathrm{Re}_\tau$-dependent behavior of the spectrum in Region I. In particular, it will be shown that the two scenarios establish theoretical links with the scaling laws in Eqs. (1) [24] and (3) [21], respectively.

### A. Scenario 1: $h_1(k_x\delta;\mathrm{Re}_\tau) > 0$ for all $\mathrm{Re}_\tau$

The first scenario assumes that the premultiplied spectrum in Region I, $h_1(k_x\delta;\mathrm{Re}_\tau)$, stops to decay to zero above a certain $\mathrm{Re}_\tau$, and it eventually loses the $\mathrm{Re}_\tau$ dependence, making $A(\mathrm{Re}_\tau)$ nonzero constant as $\mathrm{Re}_\tau \to \infty$ [see also Eq. (11b)]. This scenario is not yet supported by the DNS and experimental data in Fig. 3, as they do not show such a behavior up to $\mathrm{Re}_\tau = 20\,000$. However, here I shall assume that this may happen for very high $\mathrm{Re}_\tau$ for the purpose of understanding its theoretical consequences. In particular, this will lead to the result directly connected to the scaling law of Eq. (1).

*Theorem 1.* If $h_1(k_x\delta;\mathrm{Re}_\tau) \to \tilde{h}_1(k_x\delta) > 0$ as $\mathrm{Re}_\tau \to \infty$, then

$$\frac{\overline{u'u'}}{u_\tau^2} \to \infty \quad \text{at} \quad y^+ = c, \tag{13}$$

with a lower bound proportional to $\ln \mathrm{Re}_\tau$.

Since $\mathrm{Re}_\tau$ dependence of the spectrum originates from Region I, the given assumption effectively removes $\mathrm{Re}_\tau$ dependence of the spectrum not only in Region I but also in Region III; i.e., $h_3(k_x l;\mathrm{Re}_\tau) \to \tilde{h}_3(k_x l) > 0$ for $a/\delta \leqslant k_x \leqslant b/\delta_v$. Note that $a$ can be chosen arbitrarily. Therefore, suppose a sufficiently small $a$ is chosen for all $\mathrm{Re}_\tau$, such that $\tilde{h}_1(k_x\delta = a) = D$ where $D \leqslant \inf_{k_x} \tilde{h}_3(k_x l)$ for $a/\delta \leqslant k_x \leqslant b/\delta_v$. In this case, the contribution of the spectrum to $\overline{u'u'}/u_\tau$ in Region III must satisfy the following inequality (see also Fig. 4 for a schematic sketch):

$$\int_{\ln(al/\delta)}^{\ln(bl/\delta_v)} \tilde{h}_3(k_x l) d(\ln(k_x l)) \geqslant D \ln \mathrm{Re}_\tau + \ln\left(\frac{b}{a}\right). \tag{14}$$

This indicates that $\overline{u'u'}/u_\tau$ is unbounded as $\mathrm{Re}_\tau \to \infty$ and it has a lower bound proportional to $\ln \mathrm{Re}_\tau$ as stated above.

A stronger result can further be obtained, if the result of the classical theory of Ref. [27] is combined.

*Remark 1.* If $h_1(k_x\delta;\mathrm{Re}_\tau) \to \tilde{h}_1(k_x\delta) > 0$ as $\mathrm{Re}_\tau \to \infty$, then

$$\frac{\overline{u'u'}}{u_\tau^2} \sim \ln \mathrm{Re}_\tau \quad \text{at} \quad y^+ = c. \tag{15}$$

If $h_1(k_x\delta;\mathrm{Re}_\tau) \to \tilde{h}_1(k_x\delta)(>0)$, then one can choose $a$ so that $A(\mathrm{Re}_\tau) = A_0$ from Eq. (11b), where $A_0$ is a positive nonzero constant. Importantly, in this case, the entire theoretical setting here becomes identical to that of Ref. [27] for the logarithmic layer, if their wall-normal coordinate ($z$ in Eq. (7) in Ref. [27]) is replaced with $\delta_v$. Following the result of Ref. [27], the asymptotic form of the premultiplied spectrum in Region III for $1/\delta \ll k_x \ll b/\delta_v$ is then given by the wall-known $k_x^{-1}$ spectrum: i.e.,

$$\frac{k_x \Phi_{uu}(k_x)}{u_\tau^2} = h_3(k_x l;\mathrm{Re}_\tau) = \tilde{h}_3(k_x l) = B_0, \tag{16}$$

where $B_0$ is a positive nonzero constant. Since $A(\mathrm{Re}_\tau) = A_0$ and $B(\mathrm{Re}_\tau) \simeq B_0$ from Eq. (11d), this finally yields

$$\left.\frac{\overline{u'u'}}{u_\tau^2}\right|_{y^+=c} \simeq A_0 + C + B_0\left[\ln \mathrm{Re}_\tau + \ln\left(\frac{b}{a}\right)\right]. \tag{17}$$

Now, it is evident that the consequence of assuming non-Reynolds-number dependence of the spectrum in Region I yields the scaling in Eq. (1): comparing Eq. (1) with Eq. (17) leads to $B_s = B_0$ and $A_s = A_0 + B_0 + C\ln(b/a)$. Furthermore, $C$ in Eq. (17) (i.e., contribution from Region II in Fig. 4) is equivalent to the contribution of $f_1$ in Eq. (2a) and the rest in Eq. (17) corresponds to the contribution of $f_2$ in Eq. (2a) in the form of Eq. (2b). It is important to note that removing the $\mathrm{Re}_\tau$-dependence of the spectrum in Region I is identical to ignoring the viscosity in Regions I and III, resulting in an inviscid assumption for the motions associated with the logarithmic and outer regions, as in the theory based on attached eddy hypothesis [24].

### B. Scenario 2: $\overline{u'u'}/u_\tau^2 < \infty$ as $\mathrm{Re}_\tau \to \infty$

Although Scenario 1 in Sec. III A gives a result identical to the classical theory, the DNS and experimental data in Fig. 3 do not appear to strongly support it. Indeed, the premulitplied spectrum in Region I appears to decay slowly on increasing $\mathrm{Re}_\tau$, and it does not show any $k_x^{-1}$ behavior in Region III. This is more evident, given that the spectra from DNS and experimental data (Fig. 3) rather clearly show a $\mathrm{Re}_\tau$-independence in Region II. It rather deems possible that the premultiplied spectrum reaches zero as $\mathrm{Re}_\tau \to 0$; i.e., $h_1(k_x\delta;\mathrm{Re}_\tau) \to 0$. However, this condition alone does not provide a further insight into the scaling. This is because the scaling of $\overline{u'u'}/u_\tau^2$ essentially depends on how quickly the unknown premultiplied spectrum $h_3(k_x l;\mathrm{Re}_\tau)$ in Region III decays: see Eq. (11). A stronger assumption would therefore be needed in order to make a further theoretical progress. Fortunately, the asymptotic analysis in Ref. [21] previously showed that it is possible to have $\overline{u'u'}/u_\tau < \infty$ in boundary layers, as $\mathrm{Re}_\tau \to \infty$. This condition provides a useful guideline on how quickly $h_3(k_x l;\mathrm{Re}_\tau)$ in Region III would have to decay. If this condition is employed, then the following result is obtained.

*Theorem 2.* Suppose $B(\sigma) \in \mathbb{C}^\infty$ at $\sigma = 0$ with $\sigma = 1/\ln \mathrm{Re}_\tau$. If $\overline{u'u'}/u_\tau < \infty$ as $\mathrm{Re}_\tau \to \infty$ and either $dB/d\sigma$ or $d^2B/d\sigma^2$ is nonzero at $\sigma = 0$, then

$$\frac{\overline{u'u'}}{u_\tau^2} \sim \frac{1}{\ln \mathrm{Re}_\tau} \quad \text{at} \quad y^+ = c. \tag{18}$$

From Eq. (12a), if $\overline{u'u'}/u_\tau^2 < \infty$ is to be satisfied as $\mathrm{Re}_\tau \to \infty$, then it must be that $B(\mathrm{Re}_\tau) \to 1/(\ln \mathrm{Re}_\tau)^n$ with $n \geqslant 1$. Therefore, $1/\ln \mathrm{Re}_\tau$ now naturally emerges as a physically relevant small parameter for $\mathrm{Re}_\tau \to \infty$. Since $B(\sigma) \in \mathbb{C}^\infty$ is assumed at $\sigma = 0$, taking $\sigma$ as the small parameter of interest yields

$$B(\sigma) = B'(0)\sigma + \frac{B''(0)}{2}\sigma^2 + O(\sigma^3), \tag{19}$$

where $(\cdot)'$ for $B$ indicates differentiation with respect to $\sigma$. As $B'(\sigma)$ and $B''(\sigma)$ were assumed to be nonzero, this ultimately leads to the following scaling law:

$$\left.\frac{\overline{u'u'}}{u_\tau^2}\right|_{y^+=c} = E + \frac{F}{\ln \mathrm{Re}_\tau} + O(\sigma^2), \tag{20a}$$

where

$$E = C + B'(0), \tag{20b}$$

$$F = \frac{B''(0)}{2} + B'(0)\ln\left(\frac{b}{a}\right). \tag{20c}$$

Note that the assumption of $B'(0) \neq 0$ here is equivalent to assuming that $B(\mathrm{Re}_\tau) \to 0$ as $\mathrm{Re}_\tau \to \infty$ with the slowest possible rate to satisfy $\overline{u'u'}/u_\tau^2 < \infty$; i.e., $B(\mathrm{Re}_\tau) \to 1/\ln \mathrm{Re}_\tau$. In this case, it must be that $B'(0) > 0$, because the $B(\mathrm{Re}_\tau) > 0$ for all $\mathrm{Re}_\tau$ by definition. Since $E$ is expected be the least upper bound of $\overline{u'u'}/u_\tau^2$ as $\mathrm{Re}_\tau \to \infty$, this implies $F < 0$, resulting in the following condition for

$B''(0)$ to satisfy

$$B''(0) < -B'(0)\ln\left(\frac{b}{a}\right). \tag{21}$$

Furthermore, since $U_\infty^+ \sim \ln \mathrm{Re}_\tau$ for $\mathrm{Re}_\tau \to \infty$, Eq. (20a) is asymptotically equivalent to the result from Ref. [21] given in Eq. (3). However, unlike their analysis applicable only to boundary layers, the $1/\ln \mathrm{Re}_\tau$ scaling derived here is based on the structure of near-wall spectrum of streamwise velocity. Therefore, it is applicable to other flows, such as channel and pipe. Importantly, the framework introduced here unifies Eq. (1) from the classical attached eddy model with Eq. (3) from an asymptotic analysis. The former is a consequence of not accounting for the viscous effect of the motions from the log and outer regions. The latter is the scaling law obtained by assuming the outer-scaling part of the spectrum decays with the slowest possible rate to satisfy $\overline{u'u'}/u_\tau^2 < \infty$ for all $\mathrm{Re}_\tau$.

Finally, given the formulation introduced here, Eq. (20) is supposed to be valid strictly at a fixed inner-scaling wall-normal location; i.e., $y^+ = c$. However, the slow change of the peak wall-normal location with $\mathrm{Re}_\tau$ [19,52] can further be taken into account. Taking $\sigma(= 1/\ln \mathrm{Re}_\tau)$ as the small parameter of physical relevance, the peak streamwise turbulence intensity is written further as

$$\frac{\overline{u'u'}}{u_\tau^2}\Big|_{y^+=y_p^+} = \frac{\overline{u'u'}}{u_\tau^2}\Big|_{y^+=c} + \frac{G}{\ln \mathrm{Re}_\tau} + O(\sigma^2), \tag{22a}$$

where

$$G = \frac{1}{u_\tau^2}\frac{\partial \overline{u'u'}}{\partial y^+}\Big|_{y^+=c}\frac{dy^+}{d\sigma}\Big|_{\sigma=0}. \tag{22b}$$

Combining with Eq. (20a), this ultimately gives

$$\frac{\overline{u'u'}}{u_\tau^2}\Big|_{y^+=y_p^+} = E + \frac{H}{\ln \mathrm{Re}_\tau} + O(\sigma^2), \tag{23}$$

where $H = F + G$, and it still retains in the form of Eq. (20a).

## IV. SUMMARY AND DISCUSSIONS

Thus far, the asymptotic behavior of $\overline{u'u'}/u_\tau^2$ has been explored. The three scalings previously proposed [21,23,24] have been reviewed with their derivation process and physical justification. A new analysis has subsequently been introduced based on velocity spectrum, and two possible scenarios have been identified. Scenario 1 assumes that the outer-scaling part of the near-wall velocity spectrum reaches a nonzero constant as $\mathrm{Re}_\tau \to \infty$. The resulting scaling law was the classical $\ln \mathrm{Re}_\tau$ scaling of Ref. [24], physically consistent with the classical attached eddy model [25,27]. Scenario 2 assumes a sufficiently rapid decay of the outer-scaling part of the near-wall velocity spectrum with $\mathrm{Re}_\tau$ due to the effect of viscosity, such that $\overline{u'u'}/u_\tau^2 < \infty$ for all $\mathrm{Re}_\tau$. In this case, an $1/\ln \mathrm{Re}_\tau$ law has been obtained, and this is consistent with the result of the asymptotic analysis for the streamwise mean momentum equation in a boundary layer [21]. From now on, the theoretical results from Sec. III will further be verified using data from a high fidelity experimental measurement in Ref. [20] up to $\mathrm{Re}_\tau = 2 \times 10^4$ and from a quasilinear approximation [54] up to $\mathrm{Re}_\tau = 10^5$.

### A. Validation of theory

Here, we justify the theoretical results obtained in Sec. III. However, as shown in Fig. 1, all the existing data do not provide a clear idea on which of the scalings would fit best. Given that all the asymptotic scalings introduced in Sec. I, it is therefore necessary to have another dataset of physical relevance at higher $\mathrm{Re}_\tau$. Reference [52] recently introduced a self-consistent quasilinear

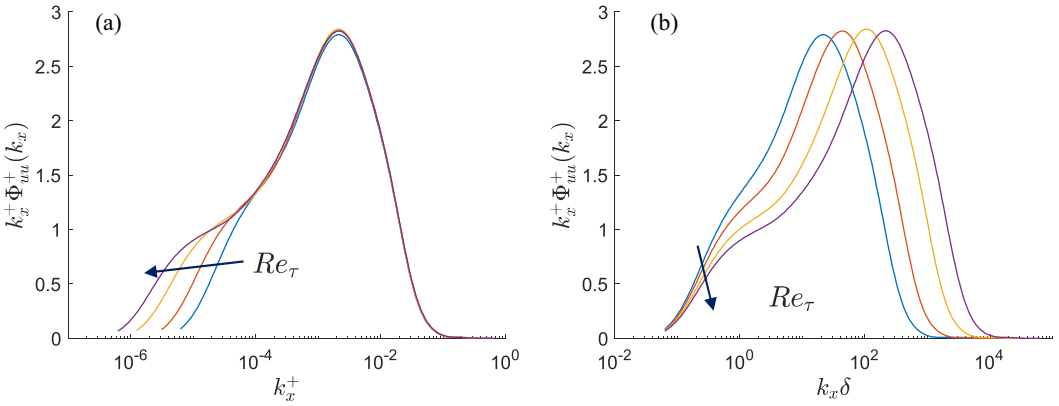


FIG. 5. Premultiplied streamwise wave number spectra of streamwise velocity at $y^+ = 20$ in channel (from a quasilinear approximation by Ref. [54]): (a) inner scaling; (b) outer scaling. Here, $\mathrm{Re}_\tau = 10\,000, 20\,000, 50\,000, 100\,000$.

approximation of the Navier-Stokes equations for channel flow. In this model, the full nonlinear mean equation is considered, while the fluctuation equations is modeled using the linearized Navier-Stokes equations where the original self-interacting nonlinear term is modeled using an eddy viscosity and stochastic forcing. The quasilinear approximation is computationally very cheap, and has been significantly extended [53,54]. It is also able to reproduce all the known scaling behaviors in a qualitative manner [53]. In this study, the data from Ref. [54] is further introduced, where streamwise wave number spectra and the corresponding turbulence intensity are computed up to $\mathrm{Re}_\tau = 10^5$. For the further details on the quasilinear model, the reader may refer to Ref. [54].

Figure 5 shows the premultiplied spectra of streamwise velocity at $y^+ = 20$ from the quasilinear approximation of Ref. [54]. It is evident that all the key scaling behaviors of the streamwise velocity spectra in with Fig. 4 are reproduced by the quasilinear approximation: For $k_x^+ \geqslant 10^{-4}$, the spectra remain universal, while for $k_x\delta \sim O(1)$, they show a decaying behavior with $\mathrm{Re}_\tau$, consistent with those from DNS and experiment in Fig. 3. The difference between the spectra from the quasilinear model and DNS/experiment is merely quantitative; for example, the peak value of the spectra from DNS and experiment is about 2.2, while that from the quasilinear approximation is about 2.8. However, as seen in the theoretical analysis in Sec. III, this is not important for the purpose of discussing the relevant scaling of data.

In Fig. 6, the scaling of the near-wall streamwise turbulence intensity from the quasilinear approximation at $y^+ = 20$ is reported. The intensity appears to follow a $\ln \mathrm{Re}_\tau$ scaling at least approximately up to $\mathrm{Re}_\tau \simeq 2 \times 10^4$, consistent with the experimental data including [20] [Fig. 6(a)]. However, similarly to the observation of Ref. [19] from the CICLoPE facility of the University of Bologna, it is seen that the intensity begins to deviate from the $\ln \mathrm{Re}_\tau$ scaling from $\mathrm{Re}_\tau \simeq 2 \times 10^4$ and this deviation becomes gradually larger, clearly visible at $\mathrm{Re}_\tau = 1 \times 10^5$. Interestingly, it appears that the same data begin to follow an $1/\ln \mathrm{Re}_\tau$ scaling for $\mathrm{Re}_\tau \geqslant 2 \times 10^4$ [Fig. 6(b)]. Note that exactly the same behavior has been observed from a computational more economical variant of the quasilinear approximation [53], where the near-wall streamwise turbulence intensity is obtained up to $\mathrm{Re}_\tau = 1 \times 10^6$.

The data shown in Figs. 1 and 6 suggest that there may be a transition in the behavior of $\overline{u'u'}/u_\tau^2$ at $\mathrm{Re}_\tau \sim O(10^4)$. To understand this behavior better, $B(\mathrm{Re}_\tau)$ [or $B(\sigma)$ with $\sigma = 1/\ln(\mathrm{Re}_\tau)$] in Eq. (12a) is further calculated using the velocity spectra from both the quasilinear approximation and the experiment of Ref. [20]. Note that $B(\mathrm{Re}_\tau)$ is the Reynolds-number dependent part of the turbulence intensity obtained in Eq. (12a), when a sufficiently small value of $a$ is chosen. Figure 7 shows $B(\mathrm{Re}_\tau)$ with respect to $\mathrm{Re}_\tau$ and $\sigma$. Both quasilinear approximation and experimental data

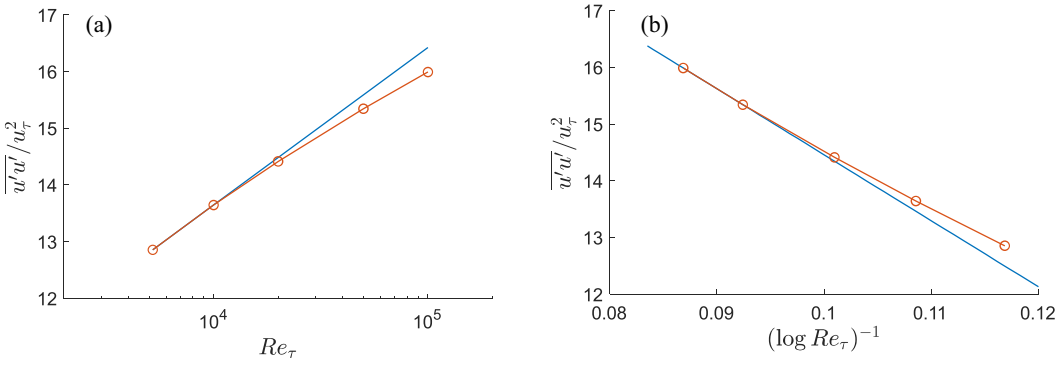


FIG. 6. Scaling of streamwise turbulence intensity at $y^+ = 20$ for the quasilinear approximation of Ref. [54] ($\mathrm{Re}_\tau = 5200, 10\,000, 20\,000, 50\,000, 100\,000$): (a) $\ln \mathrm{Re}_\tau$ scaling; (b) $1/\ln \mathrm{Re}_\tau$ scaling.

show that $B(\mathrm{Re}_\tau)$ slowly grows with $\mathrm{Re}_\tau$ up to $\mathrm{Re}_\tau \simeq 2 \times 10^4$ [Fig. 7(a)]. It is unfortunate that the experimental data above $\mathrm{Re}_\tau \simeq 2 \times 10^4$ is not available, but in $B(\mathrm{Re}_\tau)$ from the quasilinear approximation stops growing around $\mathrm{Re}_\tau \simeq 2 \times 10^4$. For $\mathrm{Re}_\tau \geqslant 5 \times 10^4$, the $B(\mathrm{Re}_\tau)$ begins to decay. This behavior is more clearly seen when $B(\sigma)$ is plotted [Fig. 7(b)]. It is worth reminding that if $\overline{u'u'}/u_\tau^2 < \infty$ as $\mathrm{Re}_\tau \to \infty$, it must be that $B(\sigma) \to 0$ as $\sigma \to 0$. The $B(\sigma)$ from the quasilinear approximation begins to exhibit this behavior around $\mathrm{Re}_\tau \simeq 2 \times 10^4$, where $\overline{u'u'}/u_\tau^2$ is approximately deviated from the $\ln \mathrm{Re}_\tau$ scaling. Furthermore, the form of $B(\sigma)$ around $\mathrm{Re}_\tau \simeq 2 \times 10^4$ suggests that it is possible to have $B''(0) < 0$. Since $\ln(b/a) < 0$ [from the choice of $a(=0.1)$ and $b \simeq 10^{-4}$ in Fig. 7] and $B'(0)$ is likely to be positive from the data, this also satisfies the condition in Eq. (21).

The examination of the quasilinear approximation data suggests that the $1/\ln \mathrm{Re}_\tau$ scaling discussed in Sec. III B is a certainly plausible scenario. However, it is seen that the experimental data [20] do not appear to cover the regime of $\mathrm{Re}_\tau$, in which the possible transition in the behavior of $B(\mathrm{Re}_\tau)$ might take place. That being said, it is important to note that the existing experimental data do not exclude the classical $\ln \mathrm{Re}_\tau$ scaling yet. Unlike the quasilinear approximation data, it is still possible that the outer-scaling part of the premultiplied spectrum, $h_1(k_x\delta; \mathrm{Re}_\tau)$, may be converged to nonzero values around a certain $\mathrm{Re}_\tau > O(10^4)$. In this case, the classical attached model is truly

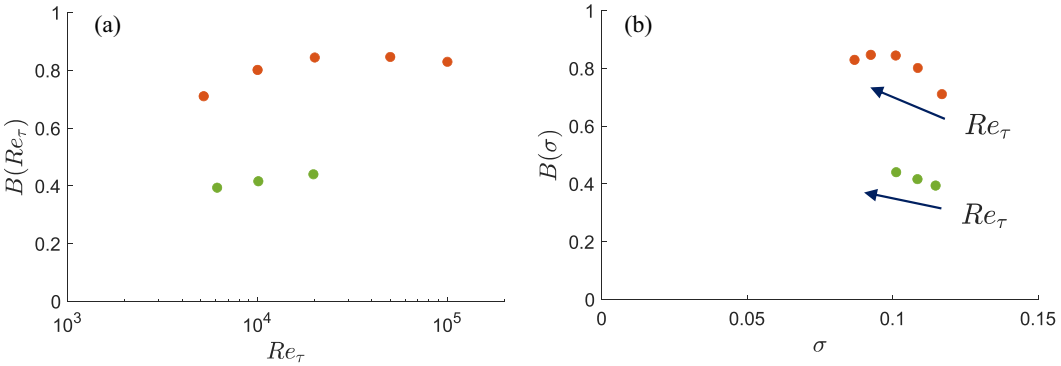


FIG. 7. $\mathrm{Re}_\tau$ dependence of $B(\mathrm{Re}_\tau)$ in Eq. (11a): (a) $B(\mathrm{Re}_\tau)$ vs $\sigma(= (1/\ln \mathrm{Re}_\tau)^{-1})$; (b) $B(\sigma)$ vs $\mathrm{Re}_\tau$. Here, data are from quasilinear approximation of Ref. [68] (orange) with $a = 0.1$ and $b \simeq 1 \times 10^{-4}$ and experiment of Ref. [20] (green) with $a = 0.2$ and $b \simeq 3 \times 10^{-4}$. Here, $\mathrm{Re}_\tau = 5200, 10\,000, 20\,000, 50\,000, 100\,000$ for the quasilinear approximation and $\mathrm{Re}_\tau = 6123, 10\,100, 19\,680$ for the experiment.

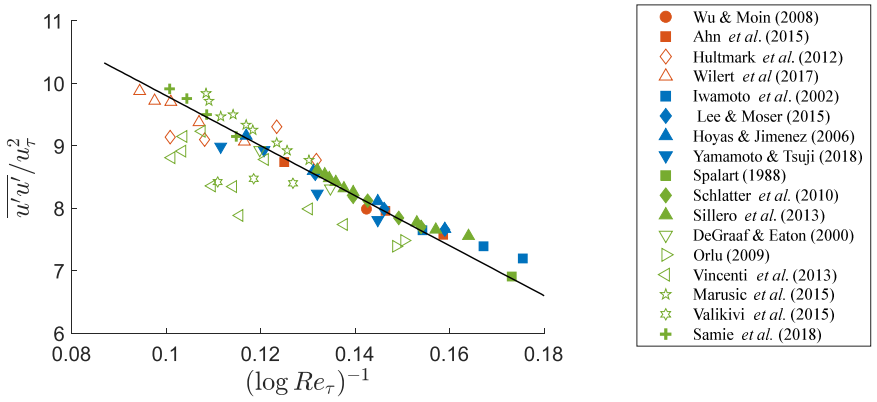


FIG. 8. Peak streamwise turbulence intensities from experiments (open symbols) and DNSs (filled symbols) with the $1/\ln \mathrm{Re}_\tau$ scaling. The curve here is given by 13.8–40/ $\ln \mathrm{Re}_\tau$.

applicable as demonstrated in Sec. III A, resulting in an indefinite logarithmic growth of turbulence intensity as $\mathrm{Re}_\tau \to \infty$. From this viewpoint, high fidelity experimental or numerical simulation data for $\mathrm{Re} > O(10^4)$ would still be required to resolve this on-going debate, although the overall trend of the existing data appears to favor the $1/\ln \mathrm{Re}_\tau$ scaling. Given the discussion above, it would finally be worth plotting all the DNS and experimental data with respect to $1/\ln(\mathrm{Re}_\tau)$, and this is shown in Fig. 8. The collapse of data with a linear fit of $1/\ln(\mathrm{Re}_\tau)$ is as good as that with the $\ln(\mathrm{Re}_\tau)$ scaling shown in Fig. 1, indicating the difficulty in identifying the correct asymptotic scaling behavior using the existing data.

### B. Inverse log law and power law

Finally, it is worth making some remarks on the $\mathrm{Re}_\tau^{-1/4}$ scaling by Ref. [23]. As discussed in Sec. I C, this scaling is based on two hypotheses which do not have strong supporting evidence yet. In particular, the specific power of $-1/4$ is derived by the timescale argument associated with the outer energy transport by the near-wall bursting, but this does not have any supporting evidence yet. We note that a similar issue has also been raised by Ref. [51], who pointed out that the $\mathrm{Re}_\tau^{-1/4}$ scaling does not naturally emerge in the Reynolds stress transport equation for $\overline{u'u'}/u_\tau^2$, whereas $1/\ln(\mathrm{Re}_\tau)$ appears naturally from the velocity spectrum and from the streamwise mean momentum equation in boundary layer [21].

In any case, here we start by assuming a power-law scaling, such that $\overline{u'u'}/u_\tau^2 \sim \mathrm{Re}_\tau^{-m}$ where $m > 0$ is a positive real number, including $m = 1/4$ of Ref. [23]. From Eq. (12a) in the present study, this case may be considered by setting $B(\mathrm{Re}_\tau) = \mathrm{Re}_\tau^{-1/4}/\ln(\mathrm{Re}_\tau)$. Then, this implies $B(\mathrm{Re}_\tau)$ admits a particular form given below:

$$B(\sigma) = \sigma e^{-\frac{m}{\sigma}}, \tag{24}$$

as $\sigma \to 0$. Since $e^{-m/\sigma}$ in Eq. (24) shall decay zero much more slowly than $\sigma$ as $\sigma \to 0$, it would be difficult to find any numerical difference between $B(\sigma) \sim \sigma$ (i.e., $1/\ln \mathrm{Re}_\tau$ scaling) and $B(\sigma) = \sigma e^{-1/(4\sigma)}$ (i.e., $\mathrm{Re}_\tau^{-1/4}$ scaling) in practice. This unfortunately implies that taking new experimental data at higher $\mathrm{Re}_\tau$ would not simply clarify the on-going issue between the different scaling laws proposed. It appears that this issue will ultimately boil down to the supporting evidence especially through advanced statistics of turbulence (e.g., full energy spectral energy balance such as Refs. [62,64] or direct examination of the bursting timescale), which can directly test the formulated hypotheses for each of the scaling arguments. In this respect, it is finally worth mentioning that the only hypothesis for the inverse log law in this study is $B(\sigma) \in \mathbb{C}^\infty$ at $\sigma = 0$, a mathematical

regularity for the solution to the Navier-Stokes equations in the limit of $\mathrm{Re}_\tau \to \infty$, and this is not a physical argument.

## ACKNOWLEDGMENTS

This work was initiated when I was visiting the Isaac Newton Institute for Mathematical Sciences at the University of Cambridge for the programme "Mathematical aspects of turbulence: Where do we stand?" (No. EP/R014604/1). I thank Prof. Rich Kerswell, who encouraged me to start this work during the visit, and Prof. I. Marusic, who shared the initial discussion of the paper.

[1] L. Prandtl, Bericht über doe emtstejimg der turbulenz, Z. Angew. Math. Mech. **5**, 136 (1925).
[2] K. R. Sreenivasan, The turbulent boundary layer, Frontiers in Expl Fluid Mech **46**, 159 (1989).
[3] S. Mochizuki and F. T. M. Nieuwstadt, Reynolds-number-dependence of the maximum in the streamwise velocity fluctuations in wall turbulence, Exp. Fluids **21**, 218 (1996).
[4] P. R. Spalart, Direct simulation of a turbulent boundary layer up to $\mathrm{Re}_\theta = 1410$, J. Fluid Mech. **187**, 61 (1988).
[5] J. C. Klewicki and R. E. Falco, On accurately measuring statistics associated with small-scale structure in turbulent boundary layers using hotwire probes, J. Fluid Mech. **219**, 119 (1990).
[6] J. M. Österlund, Experimental Studies of Zero-Pressure Gradient Tubulent Boundary Layer Flows, Ph.D. thesis, Royal Insitute of Technology (KTH), Stockholm, 1999.
[7] D. B. De graaff and J. Eaton, Reynolds-number scaling of the flat-plate turbulent boundary layer, J. Fluid Mech. **422**, 319 (2000).
[8] M. M. Metzger, J. C. Klewicki, K. L. Bradshaw, and R. Sadr, Scaling the near-wall axial turbulent stress in the zero pressure gradient boundary layer, Phys. Fluids **13**, 1819 (2001).
[9] I. Marusic, On the role of large-scale structures in wall turbulence, Phys. Fluids **13**, 735 (2001).
[10] S. Hoyas and J. Jiménez, Scaling of the velocity fluctuations in turbulent channels up to $re_\tau = 2003$, Phys. Fluids **18**, 011702 (2006).
[11] X. Wu and P. Moin, A direct numerical simulation study on the mean velocity characteristics in pipe flow, J. Fluid Mech. **608**, 81 (2008).
[12] P. Schlatter, R. Örlü, Q. Li, G. Brethouwer, J. H. M. Fransson, A. V. Johansson, P. H. Alfredsson, and D. Henningson, Turbulent boundary layers up to $\mathrm{Re}_\theta = 2500$ studied through simulation and experiment, Phys. Fluids **21**, 051702 (2009).
[13] M. Hultmark, M. Vallikivi, S. C. C. Bailey, and A. J. Smits, Turbulent pipe flow at extreme Reynolds numbers, Phys. Rev. Lett. **108**, 094501 (2012).
[14] J. A. Sillero, J. Jimenez, and R. Moser, One-point statistics for turbulent wall-bounded flows at Reynolds numbers up to $\delta^+ = 2000$, Phys. Fluids **25**, 105102 (2013).
[15] P. Vincenti, J. Klewicki, C. Morrill-Winter, C. M. White, and M. Wosnik, Streamwise velocity statistics in turbulent boundary layers that spatially develop to high Reynolds number, Exp. Fluids **54**, 1629 (2013).
[16] M. Vallikivi, M. Hultmark, and A. J. Smits, Turbulent boundary layer statistics at very high Reynolds number, J. Fluid Mech. **779**, 371 (2015).
[17] J. S. Ahn, J. H. Lee, J. Lee, J.-H. Kang, and H. J. Sung, Direct numerical simulation of a 30R long turbulent pipe flow at $re_\tau = 3008$, Phys. Fluids **27**, 065110 (2015).
[18] M. K. Lee and R. D. Moser, Direct numerical simulation of the turbulent boundary layer over a cube-roughened wall, J. Fluid Mech. **774**, 395 (2015).
[19] C. E. Willert, J. Soria, M. Stanislas, J. Klinner, O. Amili, M. Eisfelder, C. Cuvier, G. Bellani, T. Fiorini, and A. Talamelli, Near-wall statistics of a turbulent pipe flow at shear Reynolds numbers up to 40 000, J. Fluid Mech. **826**, R5 (2017).
[20] M. Samie, I. Marusic, N. Hutchins, M. K. Fu, Y. Fan, M. Hultmark, and A. J. Smits, Fully resolved measurements of turbulent boundary layer flows up to $\mathrm{Re}_\tau = 20\,000$, J. Fluid Mech. **851**, 391 (2018).

[21] P. A. Monkewitz and H. M. Nagib, Large-Reynolds-number asymptotics of the streamwise normal stress in zero-pressure-gradient turbulent boundary layers, J. Fluid Mech. **783**, 474 (2015).
[22] H. M. Nagib, P. A. Monkewitz, and K. R. Sreenivasan, Reynolds number required to accurately discriminate between proposed trends of peak normal stress in wall turbulence, Bull. Am. Phys. Soc. Q13.00006 (2022).
[23] X. Chen and K. R. Sreenivasan, Reynolds number scaling of the peak turbulence intensity in wall flows, J. Fluid Mech. **908**, R3 (2021).
[24] I. Marusic and G. J. Kunkel, Streamwise turbulent intensity formulation for flat-flate boundary layers, Phys. Fluids **15**, 2461 (2003).
[25] A. A. Townsend, *The Structure of Turbulent Shear Flow*, 2nd ed. (Cambridge University Press, Cambridge, UK, 1976).
[26] A. E. Perry and M. S. Chong, On the mechanism of turbulence, J. Fluid Mech. **119**, 173 (1982).
[27] A. E. Perry, S. Henbest, and M. S. Chong, A theoretical and experimental study of wall turbulence, J. Fluid Mech. **165**, 163 (1986).
[28] I. Marusic, J. P. Monty, M. Hultmark, and A. J. Smits, On the logarithmic region in wall turbulence, J. Fluid Mech. **716**, R3 (2013).
[29] I. Marusic and J. P. Monty, Attached eddy model of wall turbulence, Annu. Rev. Fluid Mech. **51**, 49 (2019).
[30] Y. Hwang and M. Lee, The mean logarithm emerges with self-similar energy balance, J. Fluid Mech. **903**, R6 (2020).
[31] C. D. Tomkins and R. J. Adrian, Spanwise structure and scale growth in turbulent boundary layers, J. Fluid Mech. **490**, 37 (2003).
[32] J. C. del Álamo, J. Jiménez, P. Zandonade, and R. D. Moser, Self-similar vortex clusters in the turbulent logarithmic region, J. Fluid Mech. **561**, 329 (2006).
[33] Y. Hwang and C. Cossu, Self-sustained processes in the logarithmic layer of turbulent channel flows, Phys. Fluid **23**, 061702 (2011).
[34] A. Lozano-Durán and J. Jiménez, Time-resolved evolution of coherent structures in turbulent channels: characterization of eddies and cascades, J. Fluid Mech. **759**, 432 (2014).
[35] Y. Hwang, Statistical structure of self-sustaining attached eddies in turbulent channel flow, J. Fluid Mech. **767**, 254 (2015).
[36] Y. Hwang and Y. Bengana, Self-sustaining process of minimal attached eddies in turbulent channel flow, J. Fluid Mech. **795**, 708 (2016).
[37] L. H. O. Hellström, I. Marusic, and A. J. Smits, Self-similarity of the large-scale motions in turbulent pipe flow, J. Fluid Mech. **792**, R1 (2016).
[38] J. Hwang and H. J. Sung, Wall-attached structures of velocity fluctuations in a turbulent boundary layer, J. Fluid Mech. **856**, 958 (2018).
[39] W. J. Baars and I. Marusic, Data-driven decomposition of the streamwise turbulence kinetic energy in boundary layers. Part 1: Energy spectra, J. Fluid Mech. **882**, A25 (2020).
[40] W. J. Baars and I. Marusic, Data-driven decomposition of the streamwise turbulence kinetic energy in boundary layers. Part 2: Integrated energy and $A_1$, J. Fluid Mech. **882**, A26 (2020).
[41] Y. Hwang and C. Cossu, Linear non-normal energy amplification of harmonic and stochastic forcing in the turbulent channel flow, J. Fluid Mech. **664**, 51 (2010).
[42] J. C. Klewicki, Self-similar mean dynamics in turbulent wall flows, J. Fluid Mech. **718**, 596 (2013).
[43] R. Moarref, A. S. Sharma, J. A. Tropp, and B. J. McKeon, Model-based scaling of the streamwise energy density in high-Reynolds-number turbulent channels, J. Fluid Mech. **734**, 275 (2013).
[44] B. J. McKeon, The engine behind (wall) turbulence: Perspectives on scale interactions, J. Fluid Mech. **817**, P1 (2017).
[45] B. Eckhardt and S. Zammert, Small scale exact coherent structures at large Reynolds numbers in plane Couette flow, Nonlinearity **31**, R66 (2018).
[46] Q. Yang, A. P. Willis, and Y. Hwang, Exact coherent states of attached eddies in channel flow, J. Fluid Mech. **862**, 1029 (2019).

[47] P. Doohan, A. P. Willis, and Y. Hwang, Shear stress-driven flow: The state space of near-wall turbulence as $\mathrm{Re}_\tau \to \infty$, J. Fluid Mech. **874**, 606 (2019).
[48] Y. Hwang, Mesolayer of attached eddies in turbulent channel flow, Phys. Rev. Fluids **1**, 064401 (2016).
[49] Y. Hwang, N. Hutchins, and I. Marusic, The logarithmic variance of streamwise velocity and $k^{-1}$ conundrum in wall turbulence, J. Fluid Mech. **933**, A8 (2022).
[50] N. Afzal, Fully developed turbulent flow in a pipe: An intermediate layer, Ing. arch **52**, 355 (1982).
[51] P. A. Monkewitz, Asymptotics of streamwise Reynolds stress in wall turbulence, J. Fluid Mech. **931**, A18 (2022).
[52] Y. Hwang and B. E. Eckhardt, Attached eddy model revisited using a minimal quasilinear approximation, J. Fluid Mech. **894**, A23 (2020).
[53] N. Skouloudis and Y. Hwang, Scaling of turbulence intensities up to $\mathrm{Re}_\tau = 10^6$ with a resolvent-based quasilinear approximation, Phys. Rev. Fluids **6**, 034602 (2021).
[54] J. J. Holford, M. K. Lee, and Y. Hwang, A data-driven quasilinear approximation for turbulent channel flow, J. Fluid Mech. **980**, A12 (2024).
[55] S. J. Kline, W. C. Reynolds, F. A. Schraub, and P. W. Runstadler, The structure of turbulent boundary layers, J. Fluid Mech. **30**, 741 (1967).
[56] N. Hutchins and I. Marusic, Evidence of very long meandering features in the logarithmic region of turbulent boundary layers, J. Fluid Mech. **579**, 1 (2007).
[57] R. Mathis, N. Hutchins, and I. Marusic, Large-scale amplitude modulation of the small-scale structures in turbulent boundary layers, J. Fluid Mech. **628**, 311 (2009).
[58] R. Mathis, I. Marusic, S. I. Chernyshenko, and N. Hutchins, Estimating wall-shear-stress fluctuations given an outer region input, J. Fluid Mech. **715**, 163 (2013).
[59] S. Duvvuri and B. J. McKeon, Triadic scale interactions in a turbulent boundary layer, Science **767**, R4 (2015).
[60] L. Agostini and M. Leschziner, Predicting the response of small-scale near-wall turbulence to large-scale outer motions, Phys. Fluids **28**, 015107 (2016).
[61] Q. Zhang and S. Chernyshenko, Quasi-steady quasi-homogeneous description of the scale interactions in near-wall turbulence, Phys. Rev. Fluids **1**, 014401 (2016).
[62] M. Cho, Y. Hwang, and H. Choi, Scale interactions and spectral energy transfer in turbulent channel flow, J. Fluid Mech. **854**, 474 (2018).
[63] H. Tennekes and J. L. Lumley, *A First Course in Turbulence* (MIT Press, Cambridge, MA, 1967).
[64] M. K. Lee and R. D. Moser, Spectral analysis of the budget equation in turbulent channel flows at high Reynolds number, J. Fluid Mech. **860**, 886 (2019).
[65] T. Wei, P. Fife, J. C. Klewicki, and P. Mcmurtry, Properties of the mean momentum balance in turbulent boundary layer, pipe, and channel flows, J. Fluid Mech. **522**, 303 (2005).
[66] Y. Hwang, Near-wall turbulent fluctuations in the absence of wide outer motions, J. Fluid Mech. **723**, 264 (2013).
[67] R. Deshpande, J. P. Monty, and I. Marusic, Active and inactive components of the streamwise velocity in wall-bounded turbulence, J. Fluid Mech. **914**, A5 (2020).
[68] J. J. Holford, M. K. Lee, and Y. Hwang, A data-driven quasilinear approximation for turbulent channel flow, J. Fluid Mech. **961**, A32 (2023).